J Biol Inorg Chem (2006) 11: 725–734
DOI 10.1007/s00775-006-0113-x

ORIGINAL PAPER

**Klára Nárcisz Sas · László Kovács · Ottó Zsíros
Zoltán Gombos · Győző Garab · Lars Hemmingsen
Eva Danielsen**

Fast cadmium inhibition of photosynthesis in cyanobacteria in vivo and in vitro studies using perturbed angular correlation of γ-rays

Received: 2 December 2005 / Accepted: 26 April 2006 / Published online: 5 July 2006

Abstract The effect of cadmium on the photosynthetic activity of *Synechocystis* PCC 6803 was monitored in this study. The oxygen evolving capacity of *Synechocystis* treated with 40 μM $CdCl_2$ was depressed to 10% of the maximum in 15 min, indicating that Cd^{2+} penetrated rapidly into the cells and blocked the photosynthetic activity. However, neither photosystem II (PSII) nor photosystem I (PSI) activity showed a significant short-term decrease which would explain this fast decrease in the whole-chain electron transport. Thermoluminescence measurements have shown that the charge separation and stabilization in PSII remains essentially unchanged during the first few hours following the Cd^{2+} treatment. The electron flow through PSI was monitored by following the redox changes of the P700 reaction centers of PSI. Alterations in the oxidation kinetics of P700 in the Cd^{2+}-treated cells indicated that Cd^{2+} treatment might affect the available electron acceptor pool of P700, including the CO_2 reduction and accumulation in the cells. Perturbed angular correlation of γ-rays (PAC) using the radioactive ^{111m}Cd isotope was used to follow the Cd^{2+} uptake at a molecular level. The most plausible interpretation of the PAC data is that Cd^{2+} is taken up by one or more Zn proteins replacing Zn^{2+} in *Synechocystis* PCC 6803. Using the radioactive ^{109}Cd isotope, a protein of approximately 30 kDa that binds Cd^{2+} could be observed in sodium dodecyl sulfate polyacrylamide gel electrophoresis. The results indicate that Cd^{2+} might inactivate different metal-containing enzymes, including carbonic anhydrase, by replacing the zinc ion, which would explain the rapid and almost full inhibition of the photosynthetic activity in cyanobacteria.

Keywords Cyanobacteria · *Synechocystis* sp. 6803 · Cadmium toxicity · Photosynthesis · Oxygen-evolving activity

Abbreviations BASIL: Bauers axially symmetric independent ligands · CA: Carbonic anhydrase · CCM: Carbon-concentrating mechanism · EFG: Electric field gradient · HEPES: *N*-(2-Hydroxyethyl)piperazine)-*N*′-ethanesulfonic acid · NQI: Nuclear quadrupole interaction · PAC: Perturbed angular correlation of γ-rays · PAGE: Polyacrylamide gel electrophoresis · PQ: Plastoquinone · PSI: Photosystem I · PSII: Photosystem II · Q_B: Reduced secondary quinine acceptor · Rubisco: Ribulose bisphosphate carboxylase-oxygenase · SDS: Sodium dodecyl sulfate · Tris: Tris(hydroxymethyl)aminomethane

K. N. Sas (✉) · L. Hemmingsen
Department of Natural Sciences,
Royal Veterinary and Agricultural University,
Thorvaldsensvej 40,
1871 Frederiksberg C, Denmark
E-mail: kns@kvl.dk
Fax: +45-35282350

L. Kovács · O. Zsíros · Z. Gombos · G. Garab
Institute of Plant Biology, Biological Research Center,
Hungarian Academy of Sciences, Temesvári krt 62,
Szeged 6701, Hungary

E. Danielsen
Nano Science Center, University of Copenhagen,
Universitetsparken 5,
2100 Copenhagen Ø, Denmark

Introduction

The development of human activities and industrialization has led to an increased accumulation of heavy metals in the environment. One of the most common heavy-metal pollutants is cadmium, which is not physiologically essential but is generally toxic at very low concentrations in most living organisms. The effect of Cd^{2+} has been extensively studied in bacteria and higher plants, and reviews can be found in [1–3]. Studies carried out in different plant species have revealed a wide range of different toxic effects, although the underlying molecular mechanisms are still not completely under-

stood. Cd^{2+} inhibits plant growth [4–10], can disturb oxygen metabolism [9] and reduces photosynthetic activity drastically [5, 7–19]. The effects on photosynthesis are very complex and different parts of the photosynthetic apparatus are affected by cadmium ions. Cd^{2+} influences both the light and the dark reactions of photosynthesis. It can also affect the chlorophyll content [12], trigger changes in the chloroplast membrane structure [17, 20] and inhibit carbon fixation [11, 13, 19]. Disturbances in the uptake and distribution of other micronutrients and macronutrients have also been found [21].

To study the effect of cadmium on photosynthesis, cyanobacteria can provide a very useful model because of their fast Cd^{2+} uptake, which makes it possible to monitor the path of Cd^{2+} and to distinguish between fast and delayed mechanisms caused by Cd^{2+} treatment. Certain types of bacteria can take up and accumulate heavy metals from fresh water. Removal of toxic metal ions from water by cyanobacteria has been widely studied in recent years and is a promising alternative treatment in wastewater purification [22–26]. Cyanobacteria are also suitable for biosensor applications. It was demonstrated that by monitoring oxygen evolution and its alterations due to toxic effects it is possible to obtain information about heavy-metal pollutants in sea water [27, 28].

In this study we monitored the oxygen-evolving capacity of *Synechocystis* PCC 6803 treated with 40 μM $CdCl_2$. We followed the Cd^{2+}-induced changes in the photosystem I (PSI) and photosystem II (PSII) dependent electron transport rates both in vitro and in vivo. The subcellular distribution of Cd^{2+} taken up by the cells during short (up to 15-min) exposure to Cd ions was also estimated.

In order to obtain more information about the molecular mechanisms behind the reduced photosynthetic activity, we followed the uptake of the radioactive ^{111m}Cd isotope using perturbed angular correlation of γ-rays (PAC) spectroscopy. In biological applications PAC spectroscopy is widely used to obtain information on the structure and dynamics of the metal sites of metalloproteins. Although PAC is most often used to study purified proteins, the fact that it can be applied in liquid states makes it suitable for in vivo experiments. The uptake of cadmium ions in *Synechocystis* PCC 6803 takes place very fast, within minutes, which is essential in PAC measurements owing to the short half-life (49 min) of the Cd isotope. In order to clarify the primary acting sites of Cd^{2+} inhibition, it is necessary to identify those proteins that specifically can bind Cd^{2+} in a short time. Since PAC spectroscopy is very sensitive to the coordination geometry of the metal ion, it can be used to obtain information about the immediate environment of the metal ion. We performed PAC experiments on whole cells in vivo, on cytosolic fractions and on thylakoids, at low and high pH, with and without imidazole in order to get more information about the possible Cd^{2+}-binding sites in *Synechocystis* PCC 6803.

Materials and methods

Organism and culture conditions

Synechocystis PCC 6803 cells were grown photoautotrophically at 28 °C in BG-11 medium [29] supplemented with 4 mM *N*-(2-hydroxyethyl)piperazine)-*N*′-ethanesulfonic acid (HEPES)–NaOH (pH 7.5) under continuous illumination (white light, 70 μmol photons m^{-2} s^{-1}) on a horizontal shaker.

Isolation of thylakoid membranes

Cells were harvested by centrifugation at 5,000*g* for 5 min and washed in 25 mM HEPES (pH 7.5), 10 mM EDTA buffer and then resuspended in 25 mM HEPES (pH 7.5), 1 mM phenylmethylsulfonyl fluoride, 2 mM ε-aminocaproic acid, 1 mM benzamidine. In order to break the cell walls, the suspension was mixed with an equal volume of 0.1-mm acid-washed glass beads and the suspension was vortexed in an Eppendorf tube 10 times for 1 min with 1-min interruptions for cooling on ice. The glass beads were washed with 25 mM HEPES (pH 7.5) buffer and the decanted material was spun down at 5,000*g* for 5 min to remove unbroken cells and debris. The supernatant was centrifuged at 30,000*g* for 50 min and the pelleted thylakoids were resuspended in the corresponding reaction media used in the analysis. The supernatant (cytosol) was concentrated using Centricon filters.

Measurement of photosynthetic activities

Photosynthetic oxygen-evolving activity of intact cells (from H_2O to CO_2) was measured with a Clark-type oxygen electrode (Hansatech) at saturating light intensity of 3,000 μE m^{-2} s^{-1}. The PSII and PSI dependent Hill reactions were measured on isolated thylakoid membranes resuspended in 50 mM HEPES–NaOH (pH 7.5) buffer that contained 0.4 M sucrose and 5 mM $CaCl_2$ in a Clark-type oxygen electrode at 25 °C. The PSII activity was measured in the presence of 1 mM benzoquinone. The PSI activity was determined as the oxygen uptake by the sample in the presence of 100 μM methylviologen, 15 μM *N*-(3,4-dichlorophenyl)-*N*′,*N*′-dimethylurea, 100 μM 2,6-dichlorophenolindophenol and 5 mM sodium ascorbate.

Measurement of the oxidation–reduction kinetics of P700

The light-induced redox changes of P700 were monitored by measuring the absorbance change at 820 nm using a PAM-101 chlorophyll fluorometer (Heinz Walz, Germany) equipped with an ED-820T emitter–detector

system. The same amount of sample (equivalent to 60 μg chlorophyll) was filtered onto a filter paper disk and was exposed to saturating white light provided by a KL 1500 (Schott) halogen lamp fitted with an electronic shutter for 4 s. The re-reduction kinetics was then recorded in the dark on a millisecond timescale.

Measurement of thermoluminescence

The thermoluminescence measurements were carried out in a home-built apparatus [30]. After 5-min dark adaptation at 25 °C the samples (20 μg ml^{-1} chlorophyll) were excited at −20 °C by a saturating single-turnover flash in the sample holder. Immediately after excitation, the sample was quickly cooled down to −40 °C and the emitted thermoluminescence was measured during heating of the sample in the dark at a heating rate of 20 °C min^{-1} using a Hamamatsu photomultiplier.

^{109}Cd labeling

For in vivo labeling, cells equivalent to 200 μg chlorophyll were spun down at 5,000*g* for 5 min and washed in 25 mM HEPES (pH 7.5) buffer. The cells were resuspended in 0.5 ml HEPES buffer and mixed with the same volume cadmium acetate solution containing 80 μM cadmium acetate/2 MBq $^{109}CdCl_2$ (Amersham)/0.75 M tris(hydroxymethyl)aminomethane (Tris)–HCl (pH 7.5). The cells were incubated for 30 min and washed with 25 mM HEPES (pH 7.5) buffer two times. The radioactivity of the pellet was measured using a germanium detector (Canberra). The cells were then resuspended in 10 mM EDTA, 25 mM HEPES (pH 7.5) buffer, to remove the Cd^{2+} bound to the cell wall, spun down and the activity of the pellet was measured again. The activity of the EDTA-washable fraction was considered as the Cd^{2+} bound by the cell wall. Thylakoid and cytosol fractions were also isolated and their activities were measured.

PAC spectroscopy

Using PAC spectroscopy, one can obtain information from the nuclear quadrupole interaction (NQI) between the nuclear quadrupole moment (Q) of the nucleus (in this case Cd) and the electric field gradient (EFG) originating from the surrounding charge distribution. Detailed description of the theory of PAC can be found in [31]. In biological applications, the EFG originates from the surrounding ligands at the metal sites in metal-containing proteins. PAC is mostly used to obtain structural information around the metal site, but it can be used to study dynamic effects as well [32].

PAC requires an isotope that decays by emitting two γ-rays. The PAC instrument measures the time-dependent probabilities $W(\theta,t)$ by detecting a second γ-ray at an angle θ and a time t after the first emitted γ-ray. In the case of ^{111m}Cd, the intermediate level has spin 5/2 and the energy splits into three levels under the influence of an EFG. This energy splitting of the intermediate level is reflected in the PAC spectrum. In the case of identical static, randomly oriented molecules, the probability density has the form $W(\theta,t) = e^{-t/\tau}[1 + A_{22}G_{22}(3/2\cos^2\theta - 1/2)]$, where the perturbation function $G_{22}(t)$ is given by $G_{22}(t) = a_0 + a_1\cos(\omega_1 t) + a_2\cos(\omega_2 t) + a_3\cos(\omega_3 t)$, where ω_is are the frequencies corresponding to the energy differences ($\omega_i = 2\pi\Delta E_i/h$, where h is Planck's constant) with a_i amplitudes and where the coefficient A_{22} gives the amplitude of the anisotropy in the angular correlation between the two γ-rays, and A_{22} depends only on the nuclear decay and has the value 0.18 for ^{111m}Cd [33, 34]. The correlation function $G_{22}(t)$ is found from the geometric mean of measured probabilities $\overline{W}(\theta,t)$ using

$$A_{22}G_{22}(t) = 2\frac{\overline{W}(180^\circ,t) - \overline{W}(90^\circ,t)}{\overline{W}(180^\circ,t) + 2\overline{W}(90^\circ,t)}.$$

The perturbation function is analyzed by conventional χ^2 fitting routines to equations as described in [35], yielding the NQI parameters ω_0, η and $\Delta\omega/\omega$ and τ_R. The NQI can be described by two independent parameters, $\omega_0 = |\omega_{zz}| = 12\pi|V_{zz}eQ|/40h$, where V_{zz} is the numerically largest diagonal element of the diagonalized electrical field gradient tensor $\overline{\overline{V}}$ and the asymmetry parameter η, defined as $\eta = |(V_{yy} - V_{xx})/V_{zz}|$. Each frequency is proportional to ω_0 with proportionality constants depending on η. The four amplitudes, a_0–a_3, also depend on η. $\Delta\omega/\omega$, the frequency broadening, reflects the distribution of the surroundings that the PAC isotope is in [35] and the rotational correlation time, τ_R, refers to the molecular tumbling rate, which for a spherical molecule is $\tau_R = V\xi/k_BT$ [36], where V is the molecular volume, ξ is the solution viscosity, k_B is the Boltzmann constant and T is the absolute temperature.

The PAC instrument was described in [37]. The setup consisted of six BaF_2 scintillation detectors where pairs of the detector form either 180° or 90° detector–sample–detector angles and collect correlated data in 800 time bins of 0.562 ns.

Measured PAC NQI parameters were modeled using Bauer's axially symmetric independent ligands (BASIL) model (previously denoted AOM model) [32, 38]. This is a semiempirical molecular orbital model based on observed NQIs for a series of coordination compounds of cadmium ion, and is based on the assumption that each ligand contributes to the charge distribution in a manner that is independent of the other ligands and with axial symmetry around the ligand to the metal ion bond. The NQI strengths used are listed in [32].

For the PAC experiments, thylakoid membranes were resuspended to approximately 0.25 ml in 25 mM HEPES (pH 7.5) buffer and 30 μl 4 μM cold cadmium acetate and 10 μl $^{111}CdCl_2$ dissolved in metal-free water was added. The sample was incubated for 30–60 min in

the dark, then spun down for 50 min at 30,000*g* and resuspended in 25 mM HEPES (pH 7.5)/55% sucrose buffer. For pH-shift experiment the pH was adjusted by addition of 0.5 M Tris (pH 10)/55% sucrose solution.

Results

Effect of Cd ions on the photosynthetic activity of *Synechocystis* PCC 6803

The rate of the electron transport from H_2O to CO_2 during incubation with 40 μM $CdCl_2$ was measured in intact cells (Fig. 1). The oxygen-evolving capacity of cyanobacterial suspension was depressed to 10% of the untreated value in approximately 15 min, indicating that under the experimental conditions applied cadmium ions penetrate into the cells very quickly and inhibit the photosynthetic activity of *Synechocystis* within a short time. In order to localize the site of the inhibition, different sections of the electron transport chain were measured in the presence of artificial electron acceptors and donors in isolated thylakoid membranes (Fig. 1).

Neither PSII nor PSI activity showed significant short-term inhibition, from which the fast activity decrease observed in whole-chain electron transport measured in whole cells could be explained. A decline in the activity of PSI and to a smaller extent in the activity of PSII could be observed after a few hours. However, these effects cannot be related to the sharp decrease in the activity of the whole electron transport chain in whole cells upon the addition of Cd^{2+}. The observed changes can most likely be attributed to the indirect effect of Cd^{2+}, e.g., to an increased sensitivity to photoinhibition induced by a retarded electron transport.

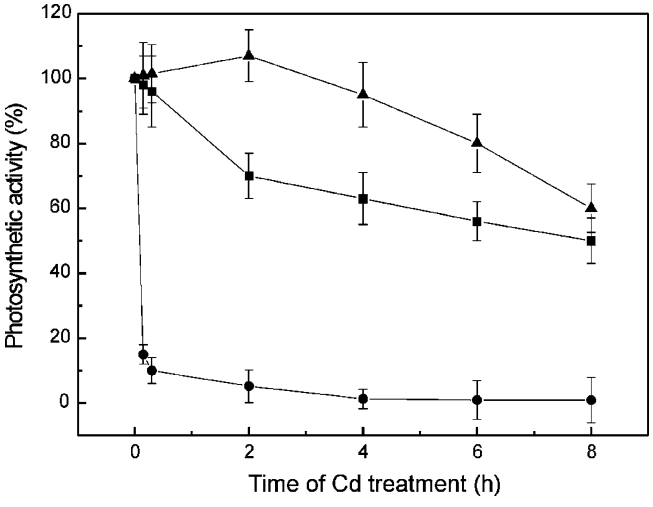

Fig. 1 Effect of 40 μM $CdCl_2$ on the rates of whole-chain photosynthetic electron transport (*filled circles*) and the photosystem I (*PSI*) (*filled squares*) and photosystem I (*PSII*) (*filled triangles*) dependent electron transport as a function of time. The rate of the whole-chain electron transport ($H_2O \rightarrow NADPH$) was measured on intact *Synechocystis* cells. The photosynthetic activities of PSI (2,6-dichlorophenolindophenol → methylviologen) and PSII ($H_2O \rightarrow$ *p*-benzoquinone.) were measured on isolated thylakoid membranes. The activities that corresponded to 100% for the intact cells, PSII and PSI Hill reactions were 480, 270 and 315 μmol O_2 mg^{-1} chlorophyll h^{-1}, respectively

Thermoluminescence

Thermoluminescence is a powerful tool for examining charge separation and the consecutive electron transfer steps in PSII. Illumination of the cyanobacterial cell suspension by a single saturating flash at −20 °C induces the B band originating from charge recombination between the S2 states of the water-splitting complex and the reduced secondary quinine acceptor (Q_B) of PSII, with a maximum at around 32 °C [39, 40]. Thermoluminescence measurements of Cd^{2+}-treated cells revealed, in perfect agreement with the PSII-dependent Hill reaction measurements (Fig. 1), that charge separation and stabilization in PSII are not affected for several hours after Cd^{2+} treatment and marked inhibition could only be observed after more than 8 h of incubation (Fig. 2).

The fact that both the intensity of the B band and its maximum temperature appear similar after several hours of Cd^{2+} treatment testify that the redox function of PSII, the water splitting and the reduction of Q_B are not affected directly by Cd^{2+} treatment.

Oxidation–reduction kinetics of P700

In order to establish the PSI activity of *Synechocystis* cells, electron flow through PSI was monitored by

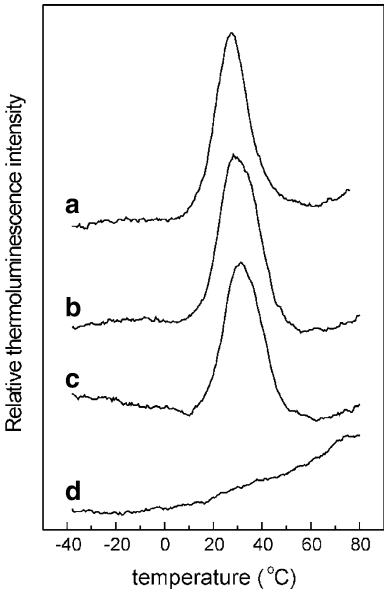

Fig. 2 Flash-induced thermoluminescence curves of *Synechocystis* cells before addition of 40 μM $CdCl_2$ (*a*) and after 2 h (*b*), 8 h (*c*) and 24 h (*d*) of $CdCl_2$ treatment. The measurements were carried out at 20 μg ml^{-1} chlorophyll concentrations following a single turnover saturating flash at −20 °C

following the redox changes of the P700 reaction centers of PSI, measured via the absorbance change at 820 nm in intact cells. Figure 3, spectrum a shows the oxidation–reduction kinetics transients of P700 upon white-light illumination for 4 s in control and Cd^{2+}-treated cells. In the untreated cell, the oxidation of P700 displays complex kinetics before it reaches the final steady-state level, as observed in many species of algae [41]. The main features of this oxidation kinetics can be described by a rapid initial decrease in the absorption connected with the fast photooxidation of P700, followed by an almost complete, transient re-reduction, and then a second, slow oxidation to the final level. The transient reduction is caused by the electron flow from the reduced intersystem electron transport components, such as cytochrome c_{553}, plastocyanin, the cytochrome b_6/f complex and the plastoquinone (PQ) pool. The slow oxidation of P700 reflects the depletion of this electron pool as a consequence of the rate-limiting step of PQH_2 oxidation at the cytochrome b_6/f complex. The dark reduction of $P700^+$ by intersystem electron transfer components after illumination follows first-order kinetics, in accordance with a single rate-limiting step between the two photosystems [42].

The oxidation of P700 in the Cd^{2+}-treated cells follows markedly different kinetics. After a short incubation in the presence of 40 μM $CdCl_2$ only the fast, transient oxidation can be observed, which is followed by a complete re-reduction and the P700 remains in a reduced state despite continuous illumination. No significant further reduction can be obtained by switching off the light (Fig. 3, spectrum b). This indicated that P700 was already completely re-reduced during the previous illumination, most likely by PSII electrons.

These data strongly suggest that, in contrast to the untreated cells, upon Cd^{2+} treatment the rate-limiting step is to be found on the acceptor side of PSI, rather than at the cytochrome b_6/f complex, i.e., at the reducing side of P700. Since no such limitation is seen in thylakoids in the presence of methylviologen, it seems plausible that the acceptor side limitation is to be found in the Calvin cycle, including its auxiliary reactions, i.e., CO_2 accumulation in the cells by carbonic anhydrases (CAs).

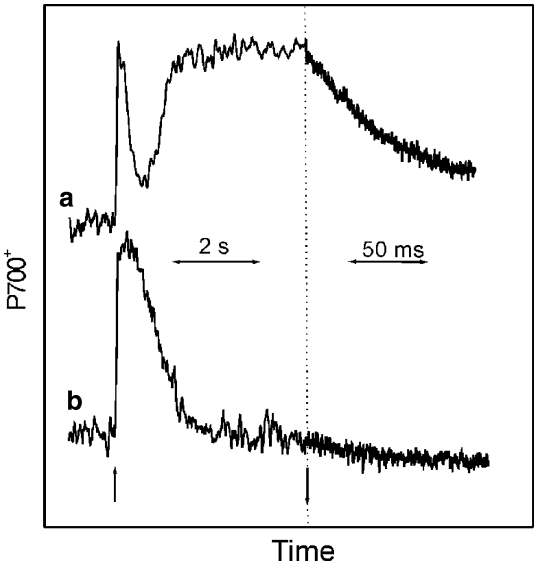

Fig. 3 Kinetics of P700 oxidation in intact cells recorded as the absorbance change at 820 nm during 4-s saturating white-light illumination and the subsequent dark relaxation period: untreated cells (*a*), cells after 15-min 40 μM $CdCl_2$ incubation (*b*); *upward and downward arrows* indicate the start and the termination of actinic illumination, respectively

^{109}Cd labeling

The identification of high molecular weight proteins to which cadmium ions can bind specifically in a short time period needs to be carried out to clarify the primer effect of this toxic heavy metal. First, we studied the distribution of Cd^{2+} in the cell. During the 5-min incubation period in the presence of ^{109}Cd, a considerable amount of Cd^{2+} was incorporated into the cells and after 30 min no further Cd^{2+} uptake was observed. After washing the cells, 65% of the total Cd^{2+} was found in the cell wall, and an estimated 19 and 16% was found in the thylakoid membranes and in the cytosol fractions, respectively. To remove the contamination from the cytosol, the thylakoid fraction was washed with 0.5 or 1 M NaCl solution. Even after 1 M NaCl washing, the radioactivity of the thylakoid fraction remained at approximately 90% of that of the unwashed sample. In order to separate the Cd^{2+}-binding proteins of the thylakoid and cytosol fractions, sodium dodecyl sulfate (SDS) polyacrylamide gel electrophoresis (PAGE) was performed. Since Cd^{2+} was released upon denaturation (in the presence of SDS and β-mercaptoethanol) of proteins, we attempted partial solubilization of thylakoid membranes and cytosolic proteins. Only after omitting the β-mercaptoethanol and lowering the SDS concentration was it possible to retain the bound Cd^{2+}. Under these conditions Cd^{2+} was mainly bound to large aggregates of proteins, but a distinct Cd^{2+}-labeled band in the range 30–35 kDa could also be identified, indicating the existence of a small protein of approximately 30–35 kDa which strongly binds Cd^{2+} in *Synechocystis* (Fig. 4).

PAC spectroscopy

The Cd^{2+} uptake in *Synechocystis* was followed by PAC spectroscopy under different conditions. Several PAC spectra were taken under every condition. The experiments under the same condition were reproducible, i.e., PAC spectra under the same conditions could be fitted with the same parameters in the limit of error. Selected PAC spectra of whole cells, on the thylakoid fraction and on the cytosolic fraction are shown in Fig. 5 with the corresponding Fourier transformations. PAC spectra of the pure thylakoid fraction measured at pH 7.5

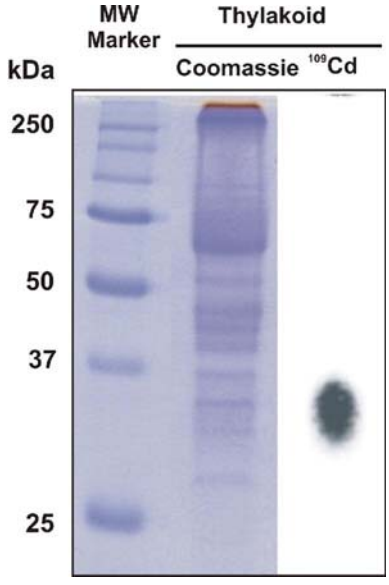

Fig. 4 Sodium dodecyl sulfate polyacrylamide gel electrophoresis (*SDS-PAGE*) analysis of ^{109}Cd-labeled thylakoid proteins. The isolated thylakoid membrane suspension was incubated with ^{109}Cd for 15 min then solubilized in Laemmli loading buffer omitting β-mercaptoethanol. A solubilized and partially denatured sample equivalent to 20 µg ml^{-1} chlorophyll was loaded onto a 15% SDS-PAGE gel. After the separation of the protein bands, the degree of ^{109}Cd incorporation was analyzed with a Storm phosphor-imager 840 (Molecular Dynamics) and the Image Quant program. The proteins were visualized by Coomassie staining

and 9.6 with and without imidazole can be seen in Figs. 6 and 7, respectively.

It can be seen in the spectra that Cd^{2+} is not free in solution, and thus is most likely bound to a molecule(s) in *Synechocystis*. Free Cd^{2+} would be seen as an additional exponential decay in the PAC spectra.

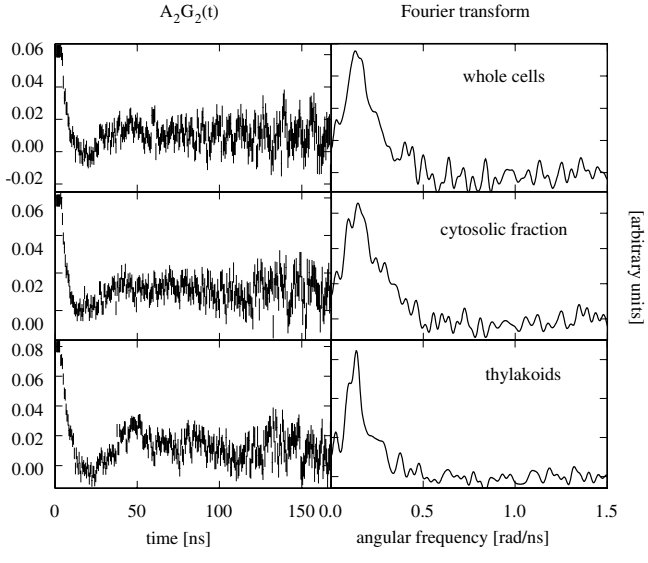

Fig. 5 Perturbation functions and Fourier transforms of ^{111m}Cd perturbed angular correlation of γ-rays (*PAC*) spectra of whole cells, purified thylakoids and cytosolic fractions at pH 7.5

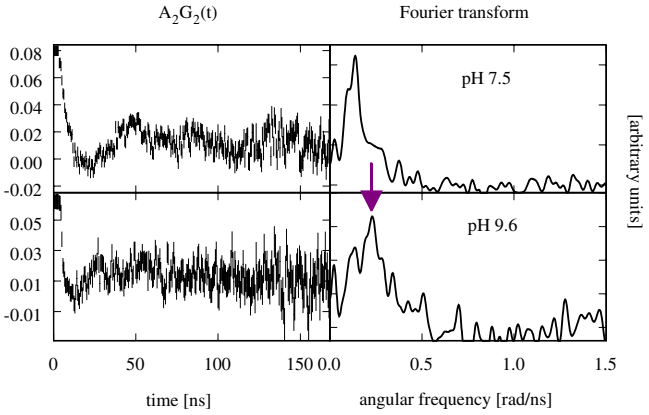

Fig. 6 Perturbation functions and Fourier transforms of ^{111m}Cd PAC spectra of purified thylakoids at pH 7.5 and 9.6

The spectra also indicate that Cd^{2+} is specifically bound to proteins in *Synechocystis*, since unspecific binding, owing to many different metal-binding sites, would not lead to distinguishable peaks in the Fourier transform spectrum of the perturbation function.

After increasing the pH from 7.5 to 9.6, the PAC spectra changed significantly, as can be seen in Fig. 6. The arrow denotes the appearance of a new peak at a higher frequency in the Fourier transform. The change in the spectrum at a higher pH value and the appearance of a population with higher frequency corresponding to a larger ω_0 parameter can be explained as the ionization of one of the ligands at the binding site at higher pH.

A significant change in the PAC spectra could be observed by the addition of imidazole to the purified thylakoid sample at pH 9.6. A very broad peak at low frequency can be seen in the Fourier transform. (The peak with lower frequency is denoted by an arrow in Fig. 7.) The change in the spectrum with imidazole indicates that the Cd^{2+}-binding site(s) is accessible for the imidazole molecules; thus, either imidazole binds to the cadmium ion as an extra ligand,or it replaces one of the ligands coordinating the cadmium ion.

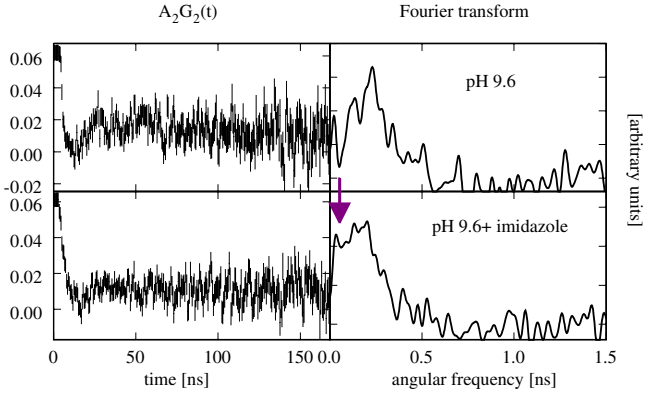

Fig. 7 Perturbation functions and Fourier transforms of ^{111m}Cd PAC spectra of purified thylakoids at pH 9.6 with and without imidazole

The results we obtained from the PAC experiments indicate that Cd^{2+} is specifically bound to metalloprotein(s) in *Synechocystis*, which could be found in the cytosol, and also in the purified thylakoid fraction. It is known that Cd^{2+} can exchange other functional divalent metal ions in metalloproteins, e.g., Ca^{2+}, Fe^{2+}, Cu^{2+} and Zn^{2+} [43–46]. The most plausible interpretation of the PAC data is that Cd^{2+} was bound to one or more metalloproteins replacing the functional divalent metal ion, and that the metal ion binding site is solvent-accessible because changes were observed upon addition of imidazole.

Discussion

The oxygen-evolving capacity of *Synechocystis* PCC 6803 treated with Cd^{2+} was depressed to 10% of the maximum within 15 min, whereas the activity of PSI and PSII reaction centers declined only slowly, and reached approximately 60% of the maximum after 8 h. These results indicate that the effect of cadmium on the two photosystems is not the main effect causing the fast decrease in photosynthetic activity.

The thermoluminescence measurements show that PSII is still completely functional 8 h after the Cd^{2+} treatment, even if there has been no photosynthetic activity at all, confirming that the redox functions of PSII, the water splitting and reduction of Q_B are not affected directly by cadmium and that the PSII inactivation does not play a role in the fast Cd^{2+} effect.

The difference in the oxidation kinetics of P700 in the PSI reaction shows that the fast effect of Cd^{2+} is related to the hindered electron flow at the acceptor side in P700. The lack of the slow oxidation phase and the complete re-reduction after illumination indicate that we have to search for the location of the site affected by the Cd^{2+} in the electron transport chain at the acceptor side of P700 and in the linked reactions including the Calvin cycle and the reactions involved in CO_2 accumulation mechanisms.

SDS-PAGE analysis indicated that a protein of approximately 30 kDa binds Cd^{2+} in *Synechocystis*.

In the PAC experiments, we could follow Cd^{2+} binding specifically to proteins in a very short time (within 30 min). The PAC data indicate that Cd^{2+} occupies the metal-binding sites in metalloprotein(s), which could be found in the cytosol as well as in the thylakoid fraction.

The relatively low frequencies in the Fourier transforms indicate that the ligands binding to the cadmium ion either have very low partial NQI frequencies or the arrangement of the ligands is very symmetric around the metal site. The change of the PAC spectra at high pH indicates the pH-induced ionization of one of the metal-binding ligands. The effect of imidazole on the PAC spectra shows that the metal-binding site is accessible to imidazole. Thus, it seems that the metal site is solvent-accessible, and therefore the change in the PAC spectra with pH may be due to the deprotonation of a metal-bound water molecule. This pK_a in the range 8–10 for a cadmium-bound water molecule at a protein metal site is not unexpected, and has been observed for CA, carboxypeptidase and alcohol dehydrogenase [47–50].

From the experimental results we can conclude that the fast cadmium effect in *Synechocystis* is related to the replacement of the functional divalent metal ion in metalloprotein(s) having a function in the photosynthetic process; in the electron transport chain at the acceptor side of P700 or in the linked reactions including the Calvin cycle and the reactions involved in CO_2 accumulation mechanisms. While it is possible that in the PAC experiments other metalloproteins bind cadmium ion as well, the only consistent interpretation of the results is that the inhibition of photosynthesis is related to the inactivation of a metalloprotein(s) observed in the PAC spectra.

Because of their high similarity in the electron shell configuration and the same formal charge, it seems likely that cadmium ions replace zinc ions [51], which are essential metal ions having functional and structural roles in many proteins. A possible interpretation of the PAC data is that Cd^{2+} is bound to one or more Zn^{2+}-containing metalloproteins replacing Zn^{2+} at the metal-binding site. Other divalent metal ions, such as Cu^{2+} or Fe^{2+}, could also be replaced by Cd^{2+}, but because of the fast exchange, it is most probable that zinc proteins were observed in the PAC spectra. It was reported that one of the main toxic effects of heavy metals on zinc-finger proteins involves the displacement of zinc by other transition metals, like Cd^{2+}, Co^{2+} or Pb^{2+} [44, 45, 52].

The genome of *Synechocystis* PCC 6803 is known, which makes it possible to search for metalloproteins and identify the zinc protein(s), which can be affected by the Cd^{2+} treatment (http://www.kazusa.or.jp/cyanobase/Synechocystis/index.html). The key roles of some trace metals in the photosynthetic processes are well known [53]. Among the metalloproteins having a function in the photosynthetic process we can find CA and in some organisms copper/zinc superoxide dismutase, which contains the zinc ion. The fact that *Synechocystis* PCC 6803 lacks copper/zinc superoxide dismutase but has manganese- and iron-containing superoxide dismutase restricts the possibilities to CAs.

CAs are widely spread enzymes, catalyzing the reversible hydration of CO_2, a reaction underlying diverse physiological processes: $CO_2 + H_2O \Leftrightarrow HCO_3^- + H^+$ [54–56]. CAs can be divided into three main classes (α, β, γ) that evolved independently and have no sequence homology. All three types have been found in different types of cyanobacteria [57], but a search of the entire genome of *Synechocystis* PCC 6803 revealed that this cyanobacterium lacks a gene encoding α-type CAs. However, the presence of genes encoding amino acid sequences similar to those of the β- and γ-type CAs in other organisms suggests the presence of β- and γ-type CAs in *Synechocystis* PCC 6803.

The location and the possible functions of CAs in the photosynthetic process are poorly understood, but it is known that their function is related to the CO_2-concentrating mechanism (CCM) in photosynthetic cells [58–63]. CAs have been found in the cytosol and in carboxysomes (ribulose bisphosphate carboxylase-oxygenase, Rubisco, containing microcompartments within the cell), but CA activity in the thylakoid has been identified in cyanobacteria, green algae and higher plants as well [61, 64–67]. CAs in the carboxysomes are thought to be necessary in the accumulation of HCO_3^- within the cell and provide an ample supply of CO_2 for Rubisco, the primary carboxylating enzyme in the Calvin cycle. A *Synechocystis* PCC 6803 mutant lacking carboxysomal CA showed drastically reduced photosynthetic activity [68]. The functions of the thylakoid-associated CA are controversial but it is known that lack of thylakoid-associated CA activity inhibits the photosynthetic activity as well. It was also shown in *Ceratophyllum demersum* L., a free-floating freshwater macrophyte, that cadmium toxicity leads to the loss of the CA activity [69]. It was reported that short-term transport of cadmium into cells of *Synechocystis aquatilis* inhibited CA activity and photosynthetic O_2 evolution [70]. It is also known that α-type CA from bovine binds Cd^{2+} as strongly as Zn^{2+}, but shows no catalytic activity at physiological pH values [71, 72]. A high Cd^{2+} concentration inhibited CA from *Chlamydomonas reinhardtii* [73] and *Chasmagnathus granulata* [74] as well.

The structure of the potential β- and γ-type CAs in *Synechocystis* PCC 6803 are not known but because of the conserved amino acid residues at the active site of the enzyme, it is assumed that the type and the arrangement of the coordinating ligands of the Zn^{2+} is identical or highly similar to that of known structures. In β-type CAs the Zn-coordinating ligands are two cysteine, one histidine and one aspartic acid residues, whereas in the γ-type CAs three histidine ligands are conserved.

In the PAC experiments we could identify proteins with relatively low NQI frequencies. In the case of the γ-type CA of *Methanosarcina thermophila* [75], the NQI parameters predicted by the BASIL model are very close to the observed values. Figure 8 shows the PAC signals that the BASIL model predicts for the case of one water molecule and three histidine coordinating ligands in a tetrahedral arrangement and for the case of two water molecules and three histidine ligands in a trigonal bipyramidal geometry. It can be clearly seen that three histidines with one or two water molecules can give frequencies in the Fourier transform as low as we observed in the PAC experiments. In contrast, in the case of the β-type CA from the red alga *Porphyridium purpureum R-1* [76] the frequencies in the Fourier transform of the parameter calculated using the BASIL model would be higher than we observed, because of the two cysteine, one histidine and one aspartic acid coordinating ligands in a distorted tetrahedral geometry (data not shown).

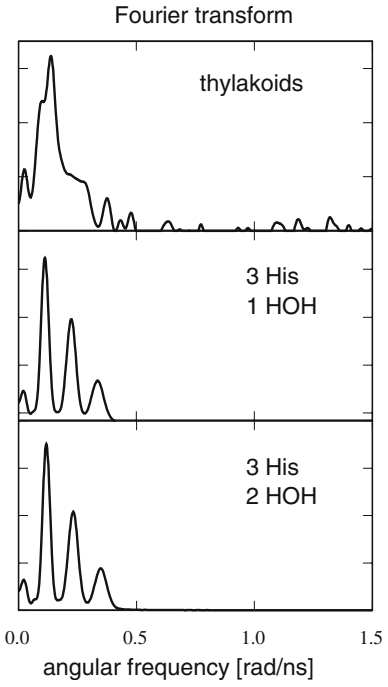

Fig. 8 Fourier transform of ^{111m}Cd PAC spectra of purified thylakoids at pH 7.5 compared with Bauer's axially symmetric independent ligands (*BASIL*) model calculations of a tetrahedral geometry of one water and three histidine ligands and of a trigonal bipyramidal geometry of two water and three histidine ligands

The PAC experiments at pH values of 7.5 and 9.6 and with added imidazole are in accordance with the assumption that CA could bind the Cd^{2+}. The change in the spectra at high pH values indicates the ionization of a ligand, in this case one of the water ligands. Earlier PAC spectra on human α-type CA, where the coordinating ligands are three histidines land one water molecule, showed a similar tendency [47–49, 77]. The change in the PAC spectra with added imidazole, which is a well-known inhibitor of CAs, was also found in the case of human α-type CA [78]. This can be interpreted as imidazole coordinating to Cd^{2+} replacing the liganding water molecule(s).

From the PAC experiments we could come to the conclusion that a CA could be one of the metalloproteins which bound Cd^{2+} in the PAC experiments. The coordination geometry and the molecular mass of 23 kDa of the γ-type CA from *Methanosarcina thermophila* support our assumption that a CA could be the target of the cadmium treatment.

We also investigated the possibility of other zinc proteins in *Synechocystis*. Some zinc proteins, such as the zinc-transport protein ZnuA, have low NQI parameter values calculated from the BASIL model because of the presence of three histidine residues and a water ligand; therefore they could bind Cd^{2+} in the PAC measurements as well. However, it is not likely that Cd^{2+} binding to zinc-transport proteins or in any other zinc-containing proteins not having a function in the

photosynthetic process could lead to the fast inhibition of photosynthesis.

We can conclude from our experiments that the primary, fast effect of the Cd^{2+} treatment that causes the drop in photosynthetic activity within minutes in *Synechocystis* PCC 6803 is most probably due to the lack of the activity of a CA involved in the CCM in the cells. The lack of enzymatic activity in CA is caused by the replacement of Zn^{2+} by Cd^{2+}. This assumption can explain all of the results discussed. Because CA is not functional in the Cd^{2+}-treated cells, CO_2 accumulation and therefore the whole Calvin cycle is hindered, which affects the electron transport chain at the acceptor side in P700. We have thus showed for the first time that PAC experiments using the radioactive ^{111m}Cd isotope can be used in in vivo experiments and in cell fractions for obtaining structural information about the metal site of the metalloproteins and thereby providing information which makes the identification of the protein(s) in the cells and cell fractions possible.

Acknowledgements We thank Marianne Lund Jensen for technical assistance. We thank also Anna Haldrup and Poul Erik Jensen for their help with biochemical facilities. This project was supported by the Danish Technical Research Council (9901473), the EU Research Training Network "Transient" (HPRN-CT-1999-00095) and the Hungarian Science Foundation OTKA (T 034188).

References

1. Das P, Samantaray S, Rout GR (1997) Environ Pollut 98:29–36
2. Prasad MNV (1995) Environ Exp Bot 35:525–545
3. Seregin IV, Ivanov VB (2001) Russ J Plant Physiol 48:523–544
4. Ali G, Srivastava PS, Iqbal M (1998) Biol Plant 41:635–639
5. Ali G, Srivastava PS, Iqbal M (2000) Biol Plant 43:599–601
6. Carrier P, Baryla A, Havaux M (2003) Planta 216:939–950
7. Di Cagno R, Guidi L, Stefani A, Soldatini GF (1999) New Phytol 144:65–71
8. Ghorbanli M, Kaveh SH, Sepehr MF (1999) Photosynthetica 37:627–631
9. Sandalio LM, Dalurzo HC, Gomez M, Romero-Puertas M, del Rio LA (2001) J Exp Bot 52:2115–2126
10. Vassilev A, Lidon FC, Matos MD, Ramalho JC, Yordanov I (2002) J Plant Nutr 25:2343–2360
11. Atri N, Rai LC (2003) J Microbiol Biotechnol 13:544–551
12. Cheng SP, Ren F, Grosse W, Wu ZB (2002) Int J Phytoremediat 4:239–246
13. Gorbunov MY, Gorbunova EA (1993) Russ J Plant Physiol 40:656–659
14. Prasad MNV, Malec P, Waloszek A, Bojko M, Strzalka K (2001) Plant Sci 161:881–889
15. Siedlecka A, Baszynski T (1993) Physiol Plant 87:199–202
16. Tumova E, Sofrova D (2002) Photosynthetica 40:103–108
17. Vassilev A, Lidon F, Scotti P, Da Graca M, Yordanov I (2004) Biol Plant 48:153–156
18. Plekhanov SE, Chemeris YK (2003) Biol Bull 30:506–511
19. Greger M, Ogren E (1991) Physiol Plant 83:129–135
20. Krupa Z (1999) Z Naturforsch C 54:723–729
21. Siedlecka A, Krupa Z (1999) Photosynthetica 36:321–331
22. Bender J, Lee RF, Phillips P (1995) J Ind Microbiol 14:113–118
23. El Enany EA, Issa AA (2000) Environ Toxicol Pharmacol 8:95–101
24. Inthorn D, Nagase H, Isaji Y, Hirata K, Miyamoto K (1996) J Ferment Bioeng 82:580–584
25. Mohamed ZA (2001) Water Res 35:4405–4409
26. Prakasham RS, Ramakrishna SV (1998) J Sci Ind Res 57:258–265
27. Campanella L, Cubadda F, Sammartino MP, Saoncella A (2001) Water Res 35:69–76
28. Tonnina D, Campanella L, Sammartino MP, Visco G (2002) Ann Chim 92:477–484
29. Allen MM (1968) J Phycol 4:1
30. Demeter S, Vass I, Horvath G, Laufer A (1984) Biochim Biophys Acta 764:33–39
31. Frauenfelder H, Steffen RM (1965) In: Siegbahn K (ed) α- β and γ-ray spectroscopy. North-Holland, Amsterdam, pp 997–1198
32. Hemmingsen L, Sas KN, Danielsen E (2004) Chem Rev 104:4027–4061
33. Butz T (1989) Hyperfine Interact 52:189–228
34. Butz T (1992) Correct Hyperfine Interact 73:387–388
35. Danielsen E, Bauer R (1990) Hyperfine Interact 62:311–324
36. Perrin F (1934) J Phys Radium 5:497–511
37. Butz T, Saibene S, Fraenzke T, Weber M (1989) Nucl Instrum Methods Phys Res A 284:417–421
38. Bauer R, Jensen SJ, Schmidt-Nielsen B (1988) Hyperfine Interact 39:203–234
39. Demeter S, Vass I (1984) Biochim Biophys Acta 764:24–32
40. Rutherford AW, Crofts AR, Inoue Y (1982) Biochim Biophys Acta 682:457–465
41. Maxwell PC, Biggins J (1977) Biochim Biophys Acta 459:442–450
42. Yu L, Zhao JD, Muhlenhoff U, Bryant DA, Golbeck JH (1993) Plant Physiol 103:171–180
43. Bonomi F, Iametti S, Kurtz DM, Ragg EM, Richie KA (1998) J Biol Inorg Chem 3:595–605
44. Hartwig A (2001) Antioxid Redox Signal 3:625–634
45. Hartwig A, Asmuss M, Blessing H, Hoffmann S, Jahnke G, Khandelwal S, Pelzer A, Burkle A (2002) Food Chem Toxicol 40:1179–1184
46. Bonomi F, Ganadu ML, Lubinu G, Pagani S (1994) Eur J Biochem 222:639–644
47. Bauer R, Limkilde P, Johansen JT (1976) Biochemistry 15:334–341
48. Bauer R, Christensen C, Johansen JT, Bethune JL, Vallee BL (1979) Biochem Biophys Res Commun 90:679–685
49. Bauer R (1985) Q Rev Biophys 18:1–64
50. Hemmingsen L, Bauer R, Bjerrum MJ, Zeppezauer M, Adolph HW, Formicka G, Cedergren-Zeppezauer E (1995) Biochemistry 34:7145–7153
51. Rensing C, Ghosh M, Rosen BP (1999) J Bacteriol 181:5891–5897
52. Kopera E, Schwerdtle T, Hartwig A, Bal A (2004) Chem Res Toxicol 17:1452–1458
53. Raven JA, Evans MCW, Korb RE (1999) Photosynth Res 60:111–149
54. Lindskog S (1997) Pharmacol Ther 74:1–20
55. Moroney JV, Bartlett SG, Samuelsson G (2001) Plant Cell Environ 24:141–153
56. Smith KS, Ferry JG (2000) FEMS Microbiol Rev 24:335–366
57. So AKC, Espie GS (2005) Can J Bot 83:721–734
58. Kaplan A, Reinhold L (1999) Annu Rev Plant Physiol Plant Mol Biol 50:539–570
59. Badger MR (2003) Photosynth Res 77:83–94
60. Badger MR, Price GD (2003) J Exp Bot 54:609–622
61. Hanson DT, Franklin LA, Samuelsson G, Badger MR (2003) Plant Physiol 132:2267–2275
62. Smith EC, Griffiths H (2000) New Phytol 145:29–37
63. Thoms S, Pahlow M, Wolf-Gladrow DA (2001) J Theor Biol 208:295–313
64. Moskvin OV, Shutova TV, Khristin MS, Ignatova KL, Villarejo A, Samuelsson G, Klimov VV, Ivanov BN (2004) Photosynth Res 79:93–100
65. Stemler AJ (1997) Physiol Plant 99:348–353
66. van Hunnik E, Sultemeyer D (2002) Funct Plant Biol 29:243–249
67. Villarejo A, Shutova T, Moskvin O, Forssen M, Klimov VV, Samuelsson G (2002) EMBO J 21:1930–1938

68. So AKC, John-McKay M, Espie GS (2002) Planta 214:456–467
69. Aravind P, Prasad MNV (2004) J Anal Atom Spectrom 19:52–57
70. Pawlik B, Skowronski T, Ramazanow Z, Gardestrom P, Samuelsson G (1993) Environ Exp Bot 33:331–337
71. Lindskog S, Malmstrom BG (1962) J Biol Chem 237:1129–1137
72. Lionetto MG, Caricato R, Erroi E, Giordano ME, Schettino T (2005) Int J Environ Anal Chem 85:895–903
73. Wang B, Liu CQ, Wu Y (2005) Bull Environ Contam Toxicol 74:227–233
74. Vitale AM, Monserrat JM, Castilho P, Rodriguez EM (1999) Comp Biochem Phys C 122:121–129
75. Iverson TM, Alber BE, Kisker C, Ferry JG, Rees DC (2000) Biochemistry 39:9222–9231
76. Mitsuhashi S, Mizushima T, Yamashita E, Yamamoto M, Kumasaka T, Moriyama H, Ueki T, Miyachi S, Tsukihara T (2000) J Biol Chem 275:5521–5526
77. Bauer R (1976) PhD thesis
78. Bauer R, Limkilde P, Johansen JT (1977) Carlberg Res Commun 42:325–339